RSC Advances

ROYAL SOCIETY OF CHEMISTRY

www.rsc.org/advances

Speciation and determination of inorganic arsenic species in water and biological samples by ultrasound assisted-dispersive-micro-solid phase extraction on carboxylated nanoporous graphene coupled with flow injection-hydride generation atomic absorption spectrometry

Aisan Khaligh[a], Hassan Zavvar Mousavi[a,*], Hamid Shirkhanloo[b], Alimorad Rashidi[c]

[a] *Department of Chemistry, Semnan University, Semnan 35131-1911, Iran.*

[b] *Occupational and Environmental Health Research Center (OEHRC), Iranian Petroleum* [c] *Nanotechnology Research Center, Research Institute of Petroleum Industry, Tehran 1485733111, Iran.*

[*]Corresponding author at: Department of Chemistry, Semnan University, Semnan 35131-1911, Iran.
E-mail address: hzmousavi@semnan.ac.ir, Tel.: +98 23 3366194; Fax: +98 23 3354110

Abstract

In this paper, the potential use of carboxylated nanoporous graphene (G-COOH) as nanoadsorbent was evaluated in two types of ultrasound assisted-dispersive micro-solid phase extraction (US-D-μ-SPE) for rapid speciation of trace arsenic (V) and arsenic (III) ions in natural water and human biological samples prior to determination by flow injection-hydride generation atomic absorption spectrometry (FI-HG-AAS). High sample volume-ultrasound assisted-dispersive micro-solid phase extraction (H-US-D-μ-SPE), and low sample volume-ultrasound assisted-dispersive micro-solid phase extraction (L-US-D-μ-SPE) were developed to extract the analyte through two pathways. As (V) ions were quantitatively recovered on G-COOH at pH 3.5, while the recoveries of As (III) were below 5%. Total arsenic content was determined as As (V) after oxidation of As (III) to As (V) using potassium permanganate. Finally, the concentration of As (III) was calculated by subtracting the As (V) content from total arsenic. Carboxylated nanoporous graphene was characterized by XRD, Raman, FT-IR, BET, SEM, TEM, and EDAX analysis. The reusability and adsorption capacity of the nanosorbent were also investigated. Under the optimized conditions, limits of detection and preconcentration factor for As (V) were 0.0021 μg L^{-1} and 50.3 in H-US-D-μ-SPE as well as 0.0248 μg L^{-1} and 5.1 in L-US-D-μ-SPE. The developed methods were successfully applied for speciation and determination of inorganic arsenic in natural water and human serum/urine samples.

Keywords: Arsenic; Speciation; Ultrasound-assisted dispersive-micro solid phase extraction; carboxylated nanoporous graphene; Flow injection-hydride generation atomic absorption spectrometry, Serum; Urine.

1. Introduction

The contamination of water by heavy metals through the discharge of industrial wastewater is a worldwide environmental problem[1]. Arsenic, a highly toxic pollutant, is widely dispersed in the environment, where it is introduced mainly from pesticides and fertilizers, glassware production, metallurgic industrial waste, melting and mining operations [2, 3]. Arsenic has caused a potential threat for environment safety and human health owing to its carcinogenic effects on hematopoietic system and the central nervous system, cardiovascular diseases, and dermal changes [4]. The World Health Organization (WHO) has set a permissible limit of 10 μg L^{-1} for arsenic in drinking water [4]. Background arsenic blood and urine levels range from 0.5 to 2 μg/L and 5 to 50 μg/L, respectively [5]. Inorganic forms of arsenic, arsenite (As (III)) and arsenate (As (V)), are the most toxic As species which tend to remain in the body and collect in human tissues [6]. To obtain complete information on the toxicity, mobility bioavailability, *etc.* of arsenic, it is necessary to speciate the different oxidation states [7, 8]. Herein, developing new analytical methods are needed due to the speciation information is becoming very important.

Several analytical techniques have been applied for determination of arsenic at trace levels including hydride generation atomic absorption spectrometry (HG-AAS) [9-11], electro-thermal atomic absorption spectrometry (ET-AAS) [12-14], inductively coupled plasma atomic emission spectrometry (ICP-AES) [15], and inductively coupled plasma mass spectrometry (ICP-MS) [16, 17], *etc*. However, the direct determination of arsenic in biological and environmental samples is bothersome due to low concentration levels of analytes and high levels of matrices. This is the reason why preconcentration and separation techniques are still necessary [8, 18]. Among various pretreatment methods, solid-phase extraction (SPE) has emerged as a powerful tool for the enrichment/separation and speciation of arsenic ions due to the advantages such as simplicity,

lower cost, higher enrichment factor, less consumption of organic solvents, and the ability to combine with different detection techniques whether in on-line or off-line mode [19-21]. Although SPE is being applied broadly, it suffers from certain shortcomings such as solvent loss, large secondary wastes, a long procedure, and a need for complex equipment [22].

Recently, dispersive-micro-solid phase extraction (D-μ-SPE), a rapid and simple clean-up technique, has been developed to reduce the time required for SPE operation, in which the extraction is carried out in the bulk solution [23]. This approach enables the sorbent to interact rapidly and uniformly with the all the target analytes and therefore shortens the time of sample preparation in comparison with a classical SPE. Sample clean-up and the extraction step are carried out simultaneously and so, it is suitable for the extraction in complex matrices[22, 24-27]. This technique can be further assisted by auxiliary energies such as ultrasonic (US) radiation in order to favor the kinetic of the mass-transfer process of the target analytes to the solid phase. This leads to an increment in the extraction efficiency of the technique in a minimum amount of time [26]. The nature and properties of the solid sorbent are of prime importance in D-μ-SPE. In practice, the main requirements for a solid sorbent are: (a) the fast and quantitative sorption and elution, (b) a high surface area and high capacity, and (c) high dispersibility in liquid samples [27]. Recently, nanomaterial-based D-μ-SPE as a novel SPE method aroused more and more concern of researchers [22].

Up to now, many carbon nanostructures such as carbon nanotubes [13, 27, 28], carbon dots [29], carbon nanohorns [30], carbon nanocones/disks [31], and even graphene [32-35], have been investigated as adsorbents in SPE and D-μ-SPE techniques due to their large specific surface areas, high adsorption capacity and good chemical stability. Graphene, one-atom thick sheet of sp^2 hybridized carbon atoms arranged in honeycomb lattice, has emerged as an attractive 2D

nanomaterial owing to its outstanding properties like large surface area, unique electrical, thermal, mechanical, and optical properties [36, 37]. These exceptional properties enable graphene to meet challenges within diverse areas like electronics and energy fields [38], as well as environmental applications [35, 36, 39]. Graphene has been made by different methods including chemical vapor deposition (CVD) growth on metal substrate [40], micromechanical exfoliation of graphite [41], epitaxial growth on electrically insulating surfaces such as SiC [42], aerosol pyrolysis [43] and solvothermal synthesis [44]. Unlike carbon nanotubes, both sides of the planar sheets of graphene are available for molecule adsorption. Hence, the ultrahigh specific surface area of graphene is responsible for its high adsorption capacity and high chemical activity [36]. However, adsorption of metal ions on graphene nanosheets often requires formation of hydrophobic complexes using chelating agents [32, 33, 45]. Herein, the development of functionalized graphene is recommended. Functionalization may further enhance the selectivity of SPE [35, 46].

Recently, nanoporous graphene has been synthesized by chemical vapor deposition (CVD) method and successfully been applied for the sorption of crude oil and hydrocarbons from water with respect to its large specific surface area (410 m^2 g^{-1}), high pore volume (1.17 cm^3 g^{-1}), and small pore size [47]. In the present study, the performance of carboxylated nanoporous graphene was examined as a new adsorbent for the extraction of inorganic arsenic ions without the using of chelating agent. Two US-D-μ-SPE methods were proposed in this work: L-D-μ-SPE and H-D-μ-SPE. The main aim of the present study is the use of H-D-μ-SPE and L-D-μ-SPE, both involving carboxylated nanoporous graphene, combined with FI-HG-AAS to develop new analytical methods for speciation and determination of trace As (V)/As (III) ions in water and biological samples. All main factors for the quantitative recoveries of the analyte ions were investigated and optimized. The developed methods have enough sensitively and

simplicity for determination of As (V) and As (III) ions in natural water and human serum/urine samples.

2. Experimental

2.1 Apparatus

A GBC atomic absorption spectrometer equipped with a hydride generation system (GBC 932 – HG3000-AUS, Australia), a deuterium-lamp background corrector, and As hallow cathode lamp was used throughout for arsenic determination. The operating conditions for FI-HG-AAS were listed in Table S1, ESI (Electronic supplementary information). The pH values were measured with a Metrohm pH-meter (model 744, Herisau, Switzerland) supplied with a glass-combined electrode. A Hettich centrifuge (model EBA 20, Hittech, Germany) and a Kunshan ultrasonic bath with temperature control (model KQ-100DE, Kunshan, China) were used throughout this study.

2.2 Chemical reagents and materials

The chemical compounds and reagents used in this work were of analytical grade and purchased from Merck (Darmstadt, Germany), unless otherwise stated. Ultra-pure deionized water (R≥18 MΩ cm-1) from Milli-Q plus water purification system (Millipore, Bedford, MA, USA) was used for preparing all aqueous solutions. As (III) and As (V) standard and experimental solutions were prepared daily by appropriate dilution of single element stock solutions of As (III) and As (V) (1000 mg L^{-1}, Merck) prior to analysis with US-D-μ-SPE. High purity sodium hydroxide (BioUltra grade, ≥98%, Sigma-Aldrich), ammonia (25%, Merck Millipore, Darmstadt, Germany), ethanol (absolute, Merck Millipore, Darmstadt, Germany), nitric acid (TraceSELECT® Ultra, 65-71%, Sigma-Aldrich), and hydrochloric acid (TraceSELECT® Ultra, 30-35%, Sigma-Aldrich) were used. The 0.6% (m/v) of sodium borohydride solution ($NaBH_4$) as

reducing agent was freshly prepared by dissolving the appropriate amount of $NaBH_4$ in 0.5% (m/v) of sodium hydroxide solution. The 5% (m/v) ascorbic acid (Merck) and 3% (m/v) KI (Merck) mixture solution as reducing agent and 0.01 mol L^{-1} of $KMnO_4$ solution as oxidizing agent were freshly prepared in ultra-pure water. The pH adjustments of samples were made using appropriate buffer solutions including sodium phosphate (H_3PO_4/NaH_2PO_4, 0.1 mol L^{-1}) for pH 2, sodium acetate (CH_3COONa/CH_3COOH, 1-2 mol L^{-1}) for pH 3-7, and ammonium chloride (NH_3/NH_4Cl, 0.2 mol L^{-1}) for pH 8-10. To decrease the risk of contamination, all the laboratory glassware and plastics (polypropylene) were cleaned by soaking in 10% (v/v) nitric acid for at least 24 hours and then rinsed with deionized water and dried in a clean oven prior to use. Moreover, all the experiments were performed in the clean lab.

2.3 *Synthesis and carboxylation of nanoporous graphene*

Nanoporous graphene was prepared by our special CVD (chemical vapor deposition) method in a catalytic basis [48]. The CVD technique was carried out in an electrical horizontal furnace consisting of a quartz tube (diameter 5 cm, length 120 cm). The furnace provided programmable heating up to 900–1100 ºC for 5–30 minutes. The reaction was carried out using methane as the carbon source and hydrogen as the carrier gas in a ratio of 4:1. In order to obtain pure nanoporous grapheme and remove the metal nanocatalysts, the product was stirred in 18% HCl solution for about 16 hours at an ambient temperature. The sample was then washed repeatedly with deionized water until the solution became neutral. The treated product was finally dried in oven at 100 ºC.

For carboxylation process, the as-prepared nanoporous graphene (1 g) was first mixed with a 100 mL mixture of concentrated H_2SO_4 and HNO_3 (3:1 v/v) and stirred for 10 minutes at room temperature followed by sonication at 60 ºC for 3 hours in an ultrasonic bath (40 kHz and

100 W). After cooling to room temperature, the reaction mixture was diluted with 500 ml of deionized water and then vacuum-filtered through a filter paper (0.22 μm porosity). This washing operation is repeated until the pH of the filtrate solution became the same as deionized water pH. Finally, the carboxylated nanoporous graphene was dried in oven at 60 °C.

2.4 *Characterization of the sorbent*

Raman spectroscopy using an Almega Thermo Nicolet and 532 nm Ar-ion laser excitation source was carried out to reveal the quality of the pristine and carboxylated nanoporous graphene. The morphology of the sorbent was examined using transmission electron microscopy (TEM, CM30, Philips, Netherland) and scanning electron microscopy (SEM, Phillips, PW3710, Netherland). The elemental composition of the samples was tested by energy dispersive X-ray microanalyser (EDX, QuanTax 200, Rontec, Germany) which was attached to SEM. A gas adsorption analyzer (Micromeritics ASAP 2010, Cleveland, USA) was used to measure the Brunauer-Emmett-Teller (BET) surface areas from nitrogen adsorption-desorption isotherms. Fourier transform infrared spectroscopy (FT-IR) was carried out on Bruker IFS 88 spectrometer (Bruker Optik GmbH, Ettlingen, Germany) using KBr pelleting method in the 4000–400 cm^{-1}. The carboxyl group content of the as-synthesized G-COOH was evaluated by adapting the modified Boehm titration procedure established for nanotubes [49]. To determine the total content of acidic groups, NaOH (0.05 N) was used instead of $NaHCO_3$ (0.05 N). A Metrohm pH-meter was employed to monitor the titration. The pH_{PZC} (point of zero charge) of G and G-COOH was determined using the known method as described previously for 0.15 g of the sample [50]. X-ray diffraction (XRD) patterns were recorded by X-ray diffractometer (XRD, PW 1840, Phillips, Netherland) with Cu-K_α radiation source. Graphene distance layer can be calculated based on Bragg's law [51]:

$$n\lambda = 2\,d_{(hkl)}\sin\theta \qquad (1)$$

Where λ is the wavelength of Cu Kα radiation (λ = 1.542 °A), θ is the scattering angle, *n* is an integer representing the order of the diffraction peak, *d* is the interplane distance of the lattices, and (*hkl*) are Miller indices. The mean crystallite size of the powder composed of relatively perfect crystalline particles can be determined via so-called Scherrer equation [51]:

$$L_{(hkl)} = \frac{0.9\lambda}{\beta\cos\theta} \qquad (2)$$

Where L_{hkl} is the mean dimension of the crystallite perpendicular to the plane (*hkl*); and β is the integral full width at half maximum in radians. However, the number of graphene layers (N) can be obtained using the following equation [52]:

$$N = \frac{L_{hkl}}{d_{hkl}} \qquad (3)$$

2.5 *US-D-μ-SPE procedures*

The two procedures, H-US-D-μ-SPE and L-D-m-SPE, provide novel and interesting approaches using the same carboxylated nanoporous graphene for extraction of As (V) ions from water and biological samples, respectively. The experimental setup of the US-D-μ-SPE procedures is illustrated in Fig. 1.

H-US-D-μ-SPE. In this procedure a 50-mL PTFE centrifuge tube and a 5-mL mini vial (MV) equipped with a plunger involving a 200 nm regenerated cellulose membrane (RC, 25 mm) were used as extraction and elution unites, respectively. Details are as follows: a 50 mL volume of water sample containing 0.5 μg L^{-1} of As (V) and/or As (III) adjusted to optimum pH value with appropriate buffer solution was transferred into the 50 mL PTFE centrifuge tube. Then, 10 mg of carboxylated nanoporous graphene was added. The mixture was placed in ultrasonic bath for 3 minutes (40 kHz, 100 W, 25 ºC) to form a homogeneous dispersion solution

and to achieve a complete D-μ-SPE procedure. The liquid/solid phases were separated by centrifugation at 6000×g for 3 minutes. Then, 45 mL of the supernatant was aspirated with pipette and only 5 mL of the remained liquid just near the solid phase at the end of the tube was transferred to a 5-mL mini vial, after vigorously shaking for 0.5 minute in order to mix the solid/liquid phases. The mixture was easily filtered through RC membrane with press down the plunger into the mini vial. The liquid phase collected inside the plunger was discharged. The nanosorbent concentrated with the analyte ions was then rinsed with deionized water to remove interference and not absorbed analytes on solid phase. Later, the plunger was pulled up and 1000 μL of 0.5 mol L^{-1} sodium hydroxide was added to the mini vial and the As (V) ions retained on the sorbent were eluted by slowly pushing the plunger. Then, As (V) ions in the eluent was reduced to As (III) by the addition of 0.2 g of L(+) ascorbic acid, 0.12 g of KI and 3 mL of 0.5 mol L^{-1} HCl solution and waiting for 1 hour. Finally, the resulting As (III) concentration was determined by FI-HG-AAS. A blank solution was also run under the same analytical conditions without adding any analytes. The adsorbent was used freshly for blank experimental run. All the experimental data were the averages of triplicate determinations. For determination of total inorganic arsenic, 0.4 mL of 0.01 mol L^{-1} $KMnO_4$ solution in acidic medium (pH=2-3) was added to the sample solution [53]. As (III) was oxidized to As (V), then the same above procedure was repeated and total inorganic arsenic was determined. The concentration of As (III) was simply calculated by mathematically subtracting the concentration of As (V) from the total arsenic concentration.

L-US-D-μ-SPE. In this procedure a 5-mL mini vial with a plunger involving a 200 nm RC membrane (MV-RC) was used for both the extraction and elution steps. A 5 mL volume of water sample containing 0.5 μg L^{-1} of As (V) and/or As (III) ions or dilution of serum/urine sample

with deionized water (1:5) (v/v) was transferred into the 5-mL mini vial, before that the pH was adjusted to optimum value. Then 3 mg of carboxylated nanoporous graphene was added. The mixture was sonicated for 1 minute (40 kHz, 100 W, 25 ºC), and then easily filtered through RC membrane with press down the plunger into the mini vial. Further procedures were the same as those previously described for H-US-D-μ-SPE except that the elution step was done with 1000 μL of 0.3 mol L^{-1}sodium hydroxide.

<Fig. 1>

2.6 *Sampling*

Different water samples including tap water (Tehran, Iran), drinking water (Tehran, Iran), petrochemical factory wastewater (Tehran, Iran), well water (Ray, Tehran, Iran), and river water (Kan, Tehran, Iran) were collected in polyethylene bottles. Each sample was filtered through Millipore cellulose membrane filter (0.45 μm pore size) in order to remove any suspended particulate and/or insoluble materials. Serum and urine samples were taken from petrochemical workers (Tehran, Iran). Fresh serum and urine samples were kept in a refrigerator at -20 ºC until sample analysis. Working solutions were prepared by dilution of 1 mL of the serum or urine samples (with deionized water) in a 5 mL volume flask. Finally, the resulting solutions were applied in US-D-μ-SPE methods and analyzed with HG-AAS. Blank samples were also analyzed. The standard reference material (NIST SRM 2669-level 1) from the National Institute of Standard and Technology (NIST, Gaithersburg, USA) was analyzed in a similar manner according to the L-US-D-μ-SPE procedure.

3. Results and discussion

3.1 *Characterization of carboxylated nanoporous graphene*

The TEM image of carboxylated nanoporous graphene (Fig. 2a) illustrates the highly porous structure of this material. The SEM image (Fig. 2b) further confirms the highly porous morphology of the sorbent with pore sizes from 45 to 63 nm.

Powder samples were further characterized by Raman spectroscopic and X-ray diffraction (XRD) measurement. As can be seen in Fig. 3a, the pristine nanoporous graphene shows the D, G, and 2D bands at 1292.5, 1583.5, and 2551 cm^{-1}, respectively. The G band is E_{2g} mode of graphite, which is due to the sp^2-bonded carbon atoms in a two-dimensional hexagonal graphite layer, while the D band is a breathing mode of k-point phonons of A_{1g} symmetry which is attributed to the presence of amorphous or disordered carbon due to the nano-sized graphitic planes and defects on these planes [54, 55]. Fig. 3b shows the peak positions of carboxylated nanoporous graphene, with D, G and 2D bands at 1351, 1585, and 2705 cm^{-1}, respectively, which were all up-shifted compared to the pristine nanoporous graphene bands. This upshift implies p-doping due to the phonon stiffening effect from charge extraction[56]. Obviously, carboxylated nanoporous graphene shows a broad strong D band with I_D/I_G=1.54 (the intensity ratio of the D and G bands), which is greater than that for pristine graphene (I_D/I_G=1.32). This is used as an evidence of the disruption of the aromatic system of π electrons by the attached molecules and therefore confirms the functionalization of graphene [57]. The most prominent feature in the Raman spectrum of graphene is the 2D peak and the intensity ratios of the G and 2D peaks (I_{2D}/I_G) that is dependent on the layer number of graphene [58]. The significant intensity increase for the 2D band, seen in Fig. 3b for carboxylated nanoporous graphene indicates that the graphene layers were decreased possibly due to the oxidation process and steric effects of functional groups. The ratio I_{2D}/I_G of these bands for pristine and carboxylated nanoporous

graphene were equal to 0.45 and 1.14. According to I_{2D}/I_G intensity ratio[59] and X-ray results, pristine and carboxylate nanoporous graphene can have six layers and three layers, respectively.

The XRD patterns of the samples are shown in Fig 4. The structural parameters such as: 2θ plane (002), interlayer distance (d), full widths at half maximum (FWHM), crystal size and the number of graphene layers were estimated from XRD patterns and summarized in Table 1. Nanoporous graphene (Fig. 4a) shows a strong and sharp (002) peak at 2θ=29.24º (corresponding to a d-spacing of 0.30 nm), which is the characteristic peak of graphene[47] indicating that the synthesized sample is a six-layer graphene. After functionalization, the (002) peak of the resulting carboxylated nanoporous graphene (Fig. 4b) shifted to 2θ=24.26º (corresponding to a d-spacing of 0.35 nm), and became broader than that of pristine graphene. Moreover, we can see a drastic increasing in FWHM of carboxylated nanoporous graphene compared to the pristine graphene. This is as a result of the introduction of oxygenated functional groups on the graphene sheets; thus the graphene layers decreased and three-layer carboxylated nanoporous graphene was obtained.

<Figs. 2 a-b>

<Figs. 3 a-b>

<Figs. 4 a-b>

The further proofs about the functional groups are offered by the following FT-IR analysis (Fig. 5). The HNO_3-H_2SO_4 treatment produced carboxyl groups on the surface of nanoporous graphene because of oxidation, as indicated by the presence of characteristic peaks at 3430 cm^{-1} and 1725 cm^{-1} for stretching vibrations of O–H and C=O of the carboxyl groups, respectively. Also, the peak at 1123 cm^{-1} is corresponded to C–O stretching vibrations of the carboxyl/or ether groups. A band at around 1630 cm^{-1} belongs to the stretching mode of the

aromatic C=C double bond that forms the skeletal of the graphene sheets. The peak at 1459 cm^{-1} is corresponded to the C-C bending mode of the graphene sheets. The two bands at 2800–2950 cm^{-1} are attributed to C-H stretching of nanoporous graphene defects. These are in agreement with the results reported by other researchers [54, 60].

Energy dispersive X-Ray spectroscopy (EDX) data of the samples were obtained and shown graphically in Fig. 6. Compared with EDX analysis of pristine nanoporous graphene (Fig. 6a), the EDX analysis of carboxylated nanoporous graphene (Fig. 6b) shows higher amount of element of O (22.01%) originating from oxidation of graphene. Moreover, the carboxyl group content of the G-COOH and its total acid functionality were determined to be 1.45 mmol g^{-1} and 1.51 mmol g^{-1}, respectively, by modified Boehm titration. The values of total acidic sites and the carboxylic acid groups are very close; thus virtually all of the acidic sites (96%) in this sample are carboxylic acid groups. All the above results clearly confirm the successful carboxylation of graphene.

The BET surface area of carboxylated nanoporous graphene was obtained as 320 $m^2 g^{-1}$. Decreasing of the BET surface area of this sample in comparison with pristine nanoporous graphene (S_{BET}=410 $m^2 g^{-1}$) is due to the carboxylation process. For the determination of pH_{PZC} of the pristine and carboxylated nanoporous graphene the values of the final pH were plotted versus their corresponding initial pH values as shown in Figure S1 (ESI). From the graph, the value of pH_{PZC} is determined from the point where the initial pH equals the final pH. It has been found that the pH_{PZC} of pristine nanoporous graphene is 6.3 and then, it shifts to lower pH value of 4.5 for carboxylated nanoporous graphene. These results imply that the sorbents have acidic surface since the pH_{PZC} values are less than 7.

<Fig. 5>

<Figs. 6 a-b>

3.2 *Optimization of the ultrasound-assisted dispersive micro solid phase extraction conditions*

In the present study, two US-D-μ-SPE methods based on carboxylated nanoporous graphene were used for speciation of trace amounts of As (V)/As (III) in water and human biological samples, prior to their determination by FI-HG-AAS. D-μ-SPE method consists of two main steps: dispersion of the acceptor phase (G-COOH in this work) into a donor phase (sample solution) and phase separation by centrifugation. This method is presented to increase the selectivity and it can be used to increase the sensitivity by holding the target analytes on the sorbent material [61]. Ultrasonic treatment was introduced to further reduction in the extraction time of the D-μ-SPE method. In order to obtain optimum speciation conditions and maximum recoveries with good sensitivity and precision, a step-by-step optimization scheme was used and included various analytical parameters.

3.2.1 *Effect of solution pH*

The solution pH is a very important parameter in US-D-μ-SPE method, as it strongly affects the surface charge of the sorbent, the degree of ionization and speciation of the adsorbate. The effect of pH on the speciation and recoveries of As (III) and As (V) ions by pristine and carboxylated nanoporous graphene was separately studied at different pH values in the range of 2-10 by using 50 mL buffered sample solutions containing 0.5 μg L^{-1} of As (III) or As (V) ions, according to the general procedure. The results for this study were depicted in Fig. 7. Obviously, using carboxylated nanoporous graphene (pH_{PZC} = 4.5), the quantitative recovery efficiencies for As (V) were achieved as >95% in pH range of 3-4, and then the recoveries were decreased with increase in pH. Whereas, the recoveries of As (III) ions were below 5% in the pH range of 2-10.

Therefore, pH of 3.5 was selected as an optimum pH value for the speciation of As (V)/As (III) ions and solid phase extraction of the As (V) for subsequent experiments (R=98%).

The effect of solution pH can be tentatively explained by considering the surface charge of the sorbent and the distribution of As species. At low pH values (pH< pH_{PZC}), the surface of carboxylated nanoporous graphene becomes positively charged (G-$COOH_2^+$) due to the protonation reaction, and so, the increased recovery of As (V) ions is due to the strong electrostatic attraction between $H_2AsO_4^-$ (the major form of As (V) at pH 2.24–6.76) and the protonated carboxyl groups on the sorbent surface (Eq. 4). The majority of As (V) is present in neutral molecular H_3AsO_4 at pH below 2.24 [4], so, the low recovery may be attributed to physical sorption via van der Waals force, *etc.* At higher pH values (pH> pH_{PZC}), the sorbent surface becomes negatively charged (G-COO^-) and so, the decrease in the recovery efficiencies of As (V) ions is due to the electrostatic repulsion between deprotonated carboxyl groups and anionic species of As (V), i.e. $H_2AsO_4^-$, and $HAsO_4^{2-}$/ AsO_4^{3-} (the major forms of As (V) at pH 6.76–11.60) [4]. On the other hand, As (III) is present as H_3AsO_3 species at pH below 7, while the $H_2AsO_3^-$ is formed at pH above 7 and becomes the main species in solution at pH above 9.5. So, the physical sorption via van der Waals force, *etc.* is the dominating mechanism for As (III) ions at the studied pH range.

G-$COOH_2^+$ + $H_2AsO_4^-$ → G-$COOH_2^+$…. $H_2AsO_4^-$ (4)

From Fig. 7, by using pristine nanoporous graphene (pH_{PZC} = 6.3), similar observations were also obtained for As (III) ions, whereas, the recoveries of As (V) were low and maximum recoveries were less than 35% in pH range of 5-6 (pH< pH_{PZC}). This is due to the lower density of oxygen-containing functional groups on nanoporous graphene, so, the physical adsorption is the main mechanism for As (V) ions sorption. On the other hand, although both the chemical and

physical adsorption processes are responsible for the higher recovery of As (V) ions by carboxylated nanoporous graphene at the optimum pH value, but chemisorption is the dominate mechanism.

<Fig. 7>

3.2.2 *Effect of carboxylated nanoporous graphene dose*

To obtain high recovery efficiency, different doses of adsorbent were tested for their ability to extract As (V) ions from water samples. Specially, different amounts of carboxylated nanoporous graphene ranging from 2 to14 mg and 1 to 8 mg were applied in H-US-D-μ-SPE and L-US-D-μ-SPE procedures, respectively. The results show that the highest recoveries were achieved by 10 mg and 3 mg of carboxylated nanoporous graphene for the 50 mL and 5 mL model solutions, respectively (Fig. S2, ESI); these were therefore selected as optimum amounts for further experiments. This is expected because more binding sites for As ions are available at higher dosage of the adsorbent. However, increasing the adsorbent dosage above the optimum amount yielded no increase on the recovery as the surface metal ions concentration and the solution metal ions concentration came to equilibrium with each other.

3.2.3 *Effect of the type, concentration and volume of eluent*

Optimization of the elution conditions were performed in order to obtain the maximum recovery with the minimal concentration and volume of the elution solution. In order to determine the best solvent for desorption of the retained As (V) ions on carboxylated nanoporous graphene, 1000 μL of various reagent solutions (NaOH, $NH_3.H_2O$, and EtOH) with different concentrations from 0.15 to 1 mol L^{-1} were tested, according to the recommended procedures. The results were shown in Figs. 8 a-b. Among the studied solutions, especially the NaOH provided higher recovery efficiency compared to the other reagents. Quantitative recovery of As (V) ions were obtained

using 0.5-1 mol L^{-1} NaOH in H-US-D-μ-SPE and 0.3-1 mol L^{-1} NaOH in L-US-D-μ-SPE. Therefore, NaOH concentrations of 0.5 mol L^{-1} for H-US-D-μ-SPE and 0.3 mol L^{-1} for L-US-D-μ-SPE were selected as the best eluent for subsequent experiments.

<Figs. 8 a-b>

Eluent volume should reach an amount that is able to desorb analyte ions. The effect of eluent volume on the recovery of As (V) ions was also studied in the range of 100-1500 μL in both US-D-μ-SPE procedures. It was found that quantitative recoveries were obtained with 1000 μL of eluent (Fig. S3, ESI). Volumes higher than 1000 μL indicated the unnecessary dilution. Therefore, 1000 μL of eluent was used in the following experiments.

3.2.4 *Effect of sample volume*

To verify the influence of the sample volume on the recovery of As (V) ions in H-US-D-μ-SPE, a set of similar preconcentration experiments according to the general procedure were carried out employing different sample volumes of 10-100 mL, each containing 0.025 μg of As (V). As can be seen from Fig. S4 (ESI), the recoveries of As (V) ions were quantitative (98%) for sample volumes up to 50 mL. Above 50 mL the recovery decreased gradually, suggesting an incomplete retention of metal ions by the sorbent. This probably due to the sample itself act as eluent or less contact of analyte ions on sorbent. Therefore, a volume of 50 mL was selected for extraction of As (V) ions from water samples.

3.2.5 *Effect of agitation type*

Sample agitation during the adsorption can improve the extraction rate and efficiency since it enhances the diffusion of the analytes towards the sorbent; on the other hand, dispersion is one of the most important factors in the performance of the US- D-μ-SPE method [27]. Therefore, the effect of agitation type, shaker or ultrasound, on the recovery efficiencies of As (V) ions was

examined, according to the H-D-μ-SPE procedure. The results revealed that quantitative recovery was obtained using ultrasonic bath (Fig. S5, ESI). It is clear that the ultrasound agitation method increases the reactivity of chemicals and also enhances the rate of mass transfer. This fact can be related to the large contact area between dispersed sorbent and the sample solution that provides a fast achievement of the equilibrium state. So ultrasound was used as an agitation method for dispersing the carboxylated nanoporous graphene in the sample solution.

3.2.6 *Effect of ultrasound-assisted extraction time*

The optimization of ultrasonication time is crucial to achieve an efficient US- D-μ-SPE procedure. In this study, different extraction times (20-200 seconds for H-US-D-μ-SPE, and 20-100 seconds L-US-D-μ-SPE) were evaluated. As shown in Fig. 9, by increasing the ultrasonication time the relative response increases, reaching the maximum value at 60 seconds for L-US-D-μ-SPE and 180 seconds for H-US-D-μ-SPE, and then remained constant. Therefore, the ultrasonic times of 3 minutes for H-US-D-μ-SPE and 1 minute for L-US-D-μ-SPE were employed.

<Fig. 9>

3.3 *Interference study*

The accurate determination of metal ions in different sample matrix is frequently problematic due to the presence of overwhelming interfering matrix components. In order to assess the possible analytical application of the US-D-μ-SPE procedure to real samples, various interfering ions were added individually to model solutions containing 0.5 μg L^{-1} As (V), under the optimized conditions. Interfering ion concentrations causing ±5% deviation in recovery of the As (V) is considered as the tolerance limit. According to the results (Table 2), the presence of

potentially interfering ions has no considerable effect on the recovery efficiencies of As (V) ions under the selected conditions.

<Table 2>

3.4 *Reusability and adsorption capacity of the sorbent*

An ideal adsorbent should not only possess higher adsorption capability, but should also show better regeneration property, which can significantly reduce the overall cost of the adsorbent [62]. In order to examine the long term stability of carboxylated nanoporous graphene, it was subjected to several extraction and elution cycles under the optimized conditions, according to the US-D-μ-SPE procedures. The nanosorbent can be used for up to 40 adsorption–elution cycles without decrease in the recoveries of the As (V).

In order to study the adsorptive capacity of sorbent for As (V) ions, batch method was used. 0.15 g of pristine and carboxylated nanoporous graphene were separately added to 50 mL of sample solutions each containing 100 mg L^{-1} of As (V) ions at pH 3.5. After ultrasonication for 15 minutes with ultrasonic bath (40 kHz, 100 W, 25 ºC), the mixture was filtered through a 0.22 μm filter membrane (GSWP 47, Millipore, Billerica, MA). The As (V) ions remaining in the filtrate were then determined with FI-HG-AAS after reduction to As (III) by the addition of 10 mL of the solution containing 5% (m/v) ascorbic acid and 3% (m/v) KI in 100 mL deionized water together with 5 mL of concentrated HCL and waiting for 1 hour. The adsorption capacity of pristine and carboxylated nanoporous graphene for As (V) ions found to be 35.0 mg g^{-1} and 125.4 mg g^{-1}. A comparison of the maximum adsorption capacities of different adsorbents for the removal of inorganic As ions from aqueous phase was also reported in Table S2 (ESI). The variation in maximum sorption capacities between the adsorbents can be related to the type and

concentration of active sites responsible for adsorption of metal ions from the solution. Obviously, the adsorption capacity of carboxylated nanoporous graphene used in the present study is significant. This may be attributed to the effect of particle size and distribution, morphology, and surface structure of the adsorbent. Therefore, carboxylated nanoporous graphene is considered to be excellent and potential adsorbent for removal of As (V) ions from effluents.

3.5 *Analytical figures of merits*

To evaluate the developed methods (H-D-μ-SPE and L-D-μ-SPE), further experiments with regard to the linearity, limit of detection (LOD) and precision of these methods were performed at the optimized working conditions in deionized water. The results were presented in Table 2. Calibration graphs were obtained for As (V) by using two different volumes of the sample solution, namely 50 and 5 mL, in two US-D-μ-SPE methods. Herein, regression equations for the calibration curves were A= 4.7702C-0.0894 (R^2= 0.9995) and A= 0.4848C-0.0599 (R^2= 0.9997), respectively, where, A is the absorbance value and C is the original concentration (μg L^{-1}) of As (V) ions in aqueous phase. The limit of detection (LOD) was calculated as the ratio of three standard deviation of the blank signal to slope of the calibration curve (3Sb/m) for ten replicate measurements of the blank solutions (50 mL and 5 mL). The precision, expressed as a relative standard deviation (RSD) for ten replicate measurements, was evaluated with model solutions containing 0.5 μg L^{-1} of As (V). The preconcentration factor (PF) was calculated as the ratio of the slopes of calibration curves of analyte after preconcentration to that prior preconcentration. As can be seen, the detection limit decreased from 0.0248 μg L^{-1} to 0.0021 μg L^{-1} when the preconcentration factor changed from 5.1 to 50.3 in the L-D-μ-SPE and H-D-μ-SPE methods, respectively. This is due to the decrease in reproducibility when using large volumes of sample.

According to Table 3, the results show good linear ranges with low LOD and RSD (%) values as well as high PF values for determination of As (V) ions in both the US-D-μ-SPE methods. These results demonstrate high sensitivity and precision of the methods for speciaton and determination of As (V)/As (III) ions in the sample solutions either with large volume of 50 ml or small volume of 5 mL.

<Table 3>

3.6 *Comparison of the developed methods with other published methods*

A comparison of the main characteristics of the developed US-D-μ-SPE methods with some established methods for speciation and determination of A(V)/As (III) ions is given in Table S3 (ESI). It is obvious that the LOD, PF, and RSD values of the both US-D-μ-SPE methods are better than, or comparable to that reported in the literature. Beside these, the presented L-US-D-μ-SPE method with using low sample volume of 5 mL also possesses the applicable linear range. These characteristics can be of key interest in applying in biochemical and clinical studies. Higher PF values of some other works are related with higher sample volumes used in these studies.

The extraction time of both US-D-μ-SPE methods is shorter than all the other methods. The high dispersity and good permeability of carboxylated nanoporous graphene used make the extraction and elution steps easy; the sample preparation time is also short, and the extraction recovery is high. Moreover, filtering with the plunger in the mini vial is a rapid single step, reducing the sample preparation time and sample loss. Other advantages of the developed US-D-μ-SPE methods include economic consumption of small amount of sorbent per extraction

without any chelating agent together with high sorption capacities and good reusability (up to 40 cycles), as well as using minimal elution volume of 1000 μL. The use of chelating agents for adsorbing of heavy metal ions makes this procedure to be complicated and time consuming and creates channeling phenomenon. Together, these results indicate that the developed US-D-μ-SPE methods are highly sensitive techniques that can be used as cheap and rapid methods for speciation and determination of inorganic As ions in enviromental and biochemical samples.

3.7 *Analytical application*

The developed US-D-μ-SPE methods were applied for determination of As (III) and As (V) ions in some water and human biological samples. The results were presented in Table 4. The accuracy of the results was verified by analyzing the spiked samples with known As (III) and As (V) concentrations. As it can be seen from Table 4, a good agreement was obtained between the added and found analytes amount, which confirms the accuracy of the procedures and its independence from the matrix effects. The recoveries of spiked samples were higher than 95% in both the US-D-μ-SPE methods. Moreover, an analysis of urinary arsenic of frozen dried human urine (NIST, SRM 2669) was used to insure the accuracy of developed L-US-D-μ-SPE method. Spiked SRM 2669 sample was also checked. As presented in Table 5, the method was in good agreement with the certified values. A good agreement was also obtained between the added and found analytes amount. The results indicate that L-US-D-μ-SPE and H-US-D-μ-SPE methods can be reliably used for the speciation and determination of As (V)/As (III) ions in serum, urine and water samples, respectively.

<Table 4>

<Table 5>

4. Conclusions

Nanoporous graphene was prepared by special CVD method, then functionalized with carboxyl groups and finally used as US-D-μ-SPE adsorbent for speciation of trace As (V)/As (III) ions in water and biological samples by two novel methods, namely H-US-D-μ-SPE and L-US-D-μ-SPE, prior to the determination by FI-HG-AAS. The developed methods are rapid, time efficient, interference-free, and most importantly easy to prepare in-house at a reasonable cost. Low adsorbent doses are utilized in these methods without any chelating agent. This study reveals the potential of carboxalated nanoporous graphene as reusable nanoadsorbent with superior adsorption capacity. The developed methods allow us to obtain good recoveries (>97%), and reproducibility with low RSD (%) values. Low detection limits with good preconcentration factors are the main advantages of these procedures. In conclusion, the developed methods are selective and accurate and can be considered as effective sample preparation techniques for mentioned ions in real water and serum/urine samples.

Acknowledgements

The authors wish to thank Semnan University Research Council, and Iranian Petroleum Industry Health Research Institute (IPIHRI) for financial support of this work.

Supplementary Information

The supplementary information contains five figures S1-S5 (pH_{PZC} of pristine and carboxylated nanoporous graphene; effect of amount of adsorbent; effect of eluent volume; effect of sample volume; and effect of agitation type on the recovery of As (V) ions) and three Tables S1-S3 (the FI-HG-AAS conditions for arsenic determination; comparison of the adsorption capacities of

various adsorbents for removal of As ions from water samples by batch method; and comparison of the developed US-D-μ-SPE methods with other reported procedures for determination of As ions in different matrixes.).

References

1. S. Khan, Q. Cao, Y. Zheng, Y. Huang and Y. Zhu, *Environ. Pollut.*, 2008, **152**, 686.
2. P. Z. Ray and H. J. Shipley, *RSC Adv.*, 2015, **5**, 29885.
3. M. Tuzen, K. O. Saygi, I. Karaman and M. Soylak, *Food Chem. Toxicol.*, 2010, **48**, 41.
4. Y. Zhang, W. Wang, L. Li, Y. Huang and J. Cao, *Talanta*, 2010, **80**, 1907.
5. M. F. Hughes, *Environ. Health Perspect.*, 2006, 1790.
6. K. Jomova, Z. Jenisova, M. Feszterova, S. Baros, J. Liska, D. Hudecova, C. Rhodes and M. Valko, *J. Appl. Toxicol.*, 2011, **31**, 95.
7. A. A. Ensafi, A. C. Ring and I. Fritsch, *Electroanal.*, 2010, **22**, 1175.

8. H. Erdoğan, Ö. Yalçınkaya and A. R. Türker, *Desalination*, 2011, **280**, 391.

9. T.-M. Hsiung and J.-M. Wang, *J. Anal. At. Spectrom.*, 2004, **19**, 923.

10. O. D. Uluozlu, M. Tuzen, D. Mendil and M. Soylak, *Food Chem. Toxicol.*, 2010, **48**, 1393.

11. G. Lai, G. Chen and T. Chen, *Food Chem.*, 2016, **190**, 158.

12. M. Ghambarian, M. R. Khalili-Zanjani, Y. Yamini, A. Esrafili and N. Yazdanfar, *Talanta*, 2010, **81**, 197.

13. I. López-García, R. E. Rivas and M. Hernández-Córdoba, *Talanta*, 2011, **86**, 52.

14. P. Liang and R. Liu, *Anal. Chim. Acta*, 2007, **602**, 32.

15. K. Jitmanee, M. Oshima and S. Motomizu, *Talanta*, 2005, **66**, 529.

16. K. Ito, C. D. Palmer, A. J. Steuerwald and P. J. Parsons, *J. Anal. At. Spectrom.*, 2010, **25**, 1334.

17. P. Li, X.-q. Zhang, Y.-j. Chen, T.-y. Bai, H.-z. Lian and X. Hu, *RSC Adv.*, 2014, **4**, 49421.

18. M. A. Karimi, A. Mohadesi, A. Hatefi-Mehrjardi, S. Z. Mohammadi, J. Yarahmadi and A. Khayrkhah, *J. Chem.*, 2014, **2014**, 1.

19. X. Liu, T. Duan, Y. Han, X. Jia and H. Chen, *J. Anal. At. Spectrom.*, 2010, **25**, 206.

20. N. J. Simpson, *Solid-phase extraction: principles, techniques, and applications*, CRC Press, 2000.

21. Y. Jiang, Y. Wu, J. Liu, X. Xia and D. Wang, *Microchim. Acta*, 2008, **161**, 137.

22. X. Jiang, M. Wu, W. Wu, J. Cheng, H. Zhou and M. Cheng, *Anal. Method*, 2014, **6**, 9712.

23. W. H. Chung, S. H. Tzing, M. C. Huang and W. H. Ding, *J. Chinese Chem. Soc.*, 2014, **61**, 1031.

24. F. Galán-Cano, R. Lucena, S. Cárdenas and M. Valcárcel, *Microchem. J.*, 2013, **106**, 311.

25. J. M. Jiménez-Soto, S. Cárdenas and M. Valcárcel, *Anal. Chim. Acta*, 2012, **714**, 76.

26. A. R. Fontana, N. B. Lana, L. D. Martinez and J. C. Altamirano, *Talanta*, 2010, **82**, 359.

27. K. Kocot, B. Zawisza, E. Marguí, I. Queralt, M. Hidalgo and R. Sitko, *J. Anal. At. Spectrom.*, 2013, **28**, 736.

28. Y. Liu, Y. Li and L. Yang, *Microchem. J.*, 2012, **104**, 56.

29. Y. Liu, J. Hu, Y. Li, H.-P. Wei, X.-S. Li, X.-H. Zhang, S.-M. Chen and X.-Q. Chen, *Talanta*, 2015, **134**, 16.

30. S. Zhu, W. Niu, H. Li, S. Han and G. Xu, *Talanta*, 2009, **79**, 1441.

31. J. M. Jiménez-Soto, S. Cárdenas and M. Valcárcel, *J. Chromatogr., A*, 2009, **1216**, 5626.

32. Y. Wang, S. Gao, X. Zang, J. Li and J. Ma, *Anal. Chim. Acta*, 2012, **716**, 112.

33. Y. K. Wang, S. T. Gao, J. J. Ma and J. C. Li, *J. Chinese Chem. Soc.*, 2012, **59**, 1468.

34. M. Ghazaghi, H. Shirkhanloo, H. Z. Mousavi and A. M. Rashidi, *Microchim. Acta*, 2015, **182**, 1263.

35. N. Ye and P. Shi, *Sep. Purif. Rev.*, 2015, **44**, 183.

36. H. Wang, X. Yuan, Y. Wu, H. Huang, X. Peng, G. Zeng, H. Zhong, J. Liang and M. Ren, *Adv. Colloid Interface Sci.*, 2013, **195**, 19.

37. Y. Zhu, S. Murali, W. Cai, X. Li, J. W. Suk, J. R. Potts and R. S. Ruoff, *Adv. Mater.*, 2010, **22**, 3906.

38. M. D. Stoller, S. Park, Y. Zhu, J. An and R. S. Ruoff, *Nano Lett.*, 2008, **8**, 3498.

39. S. Wang, H. Sun, H.-M. Ang and M. Tadé, *Chem. Eng. J.*, 2013, **226**, 336.

40. Y. Zhang, L. Zhang and C. Zhou, *Acc. Chem. Res.*, 2013, **46**, 2329.

41. K. S. Novoselov, A. K. Geim, S. Morozov, D. Jiang, Y. Zhang, S. Dubonos, I. Grigorieva and A. Firsov, *science*, 2004, **306**, 666.

42. S. Shivaraman, R. A. Barton, X. Yu, J. Alden, L. Herman, M. Chandrashekhar, J. Park, P. L. McEuen, J. M. Parpia and H. G. Craighead, *Nano Lett.*, 2009, **9**, 3100.

43. J. Campos-Delgado, J. M. Romo-Herrera, X. Jia, D. A. Cullen, H. Muramatsu, Y. A. Kim, T. Hayashi, Z. Ren, D. J. Smith and Y. Okuno, *Nano Lett.*, 2008, **8**, 2773.

44. M. Choucair, P. Thordarson and J. A. Stride, *Nat. Nanotechnol.*, 2009, **4**, 30.

45. Y. Wang, X. Ke, X. Zhou, J. Li and J. Ma, *J. Saudi Chem. Soc.*, 2012.

46. B. Zawisza, R. Sitko, E. Malicka and E. Talik, *Anal. Method*, 2013, **5**, 6425.

47. S. Pourmand, M. Abdouss and A. Rashidi, *J. Ind. Eng. Chem.*, 2015, **22**, 8.

48. , A.M. Rashidi, Z. Hajjar, A. Ghozatllo, M. Rashtchi, Submitted to US Patent office.

49. H. Hu, P. Bhowmik, B. Zhao, M. Hamon, M. Itkis and R. Haddon, *Chem. Phys. Lett.*, 2001, **345**, 25.

50. S. M. Lee and D. Tiwari, *Chem. Eng. J.*, 2013, **225**, 128.

51. H. P. Klug and L. E. Alexander, *X-ray diffraction procedures*, John Willy & Sons Inc, New York, 1954.

52. H.-M. Ju, S.-H. Choi and S.-H. Huh, *J. Korean Phys. Soc.*, 2010, **57**, 1649.

53. L. Na, F. Maohong, J. Van Leeuwen, B. Saha, Y. Hongqun and C. Huang, *J. Environ. Sci.*, 2007, **19**, 783.

54. L. Gao, Y. Xiao, Y. Wang, X. Chen, B. Zhou and X. Yang, *Talanta*, 2015, **132**, 215.

55. H. Naeimi, A. Mohajeri, L. Moradi and A. M. Rashidi, *Appl. Surf. Sci.*, 2009, **256**, 631.

56. A. Das, S. Pisana, B. Chakraborty, S. Piscanec, S. Saha, U. Waghmare, K. Novoselov, H. Krishnamurthy, A. Geim and A. Ferrari, *Nat. Nanotechnol.*, 2008, **3**, 210.

57. J. Azizian, H. Tahermansouri, E. Biazar, S. Heidari and D. C. Khoei, *Int. J. Nanomedicine*, 2010, **5**, 907.

58. A. Ferrari, J. Meyer, V. Scardaci, C. Casiraghi, M. Lazzeri, F. Mauri, S. Piscanec, D. Jiang, K. Novoselov and S. Roth, *Phys. Rev. Lett.*, 2006, **97**, 187401.

59. A. Das, B. Chakraborty and A. Sood, *Bull. Mater. Sci.*, 2008, **31**, 579.

60. V. A. Chhabra, A. Deep, R. Kaur and R. Kumar, *Int. j. sci. emerg. technol. latest trends*, 2012, **4**, 13.

61. H. Abdolmohammad-Zadeh and Z. Talleb, *Microchim. Acta*, 2012, **179**, 25.

62. C. J. Madadrang, H. Y. Kim, G. Gao, N. Wang, J. Zhu, H. Feng, M. Gorring, M. L. Kasner and S. Hou, *ACS Appl. Mater. Inter.*, 2012, **4**, 1186.

Table 1 X-ray structural parameters of pristine and carboxylated nanoporous graphene.

samples	2θ	FWHM (º)	Layer distance (Å)	Crystal thickness (nm)	Number of layer≈
G	29.24	4.65	3.05	17.66	6

G-COOH	24.26	7.52	3.54	10.83	3

Table 2 Effect of potentially interfering ions on the recovery of As (V) ions.

Foreign ions	Concentration ratio ($C_{interferent\ ion}/C_{As}^{5+}$)	Recovery (%)

CrO_4^{2-}	200	96
$Cr_2O_7^{2-}$	180	98
MnO_4^-	220	95
Bi^{3+}, V^{5+}	500	96
Mo^{6+}	400	97
$H_2PO_4^-$	750	98
Ni^{2+}, Co^{2+}	1100	97
Hg^{2+}	350	96
Al^{3+}	800	97
Ag^+, Fe^{3+}	550	97
Cl^-, NO_3^-, SO_4^{2-}, HCO_3^-, F^-	1250	97
Cd^{2+}, Pb^{2+}	1200	96
Ca^{2+}, Mg^{2+}, Na^+, K^+, Li^+	1000	97
Zn^{2+}	450	97
Cu^{2+}	400	98

Table 3 Analytical characteristics of the developed US-D-μ-SPE methods at the optimum conditions.

Metal ions	Sample volume (mL)	Linear range (μg L^{-1})	Slope (α)	Regression coefficient (R^2)	LOD [a] (n = 10) (μg L^{-1})	RSD [b] (n = 10) (%)	PF [c]
As^{5+}	50	0.01 – 0.65	4.7702	0.9995	0.0021	3.1	50.2
As^{5+}	5	0.11 – 6.60	0.4848	0.9997	0.0248	2.6	5.1

[a] Limit of detection , [b] Relative standard deviation, [c] Preconcentration factor

Table 4 Analytical results for determination of analytes in spiked natural water samples, spiked human serum and urine samples with the developed US-D-μ-SPE methods.

Sample	Added (μg L^{-1})	Found [a] (μg L^{-1})	RSD[b] (%)	Recovery (%)

	As^{5+}	As^{3+}	As^{5+}	As^{3+}	As^{5+}	As^{3+}	As^{5+}	As^{3+}
Drinking Water	----	----	0.185±0.072	0.126±0.110	2.8	2.9	----	----
	0.1	0.1	0.284±0.063	0.228±0.231	2.7	3.2	99	102
Tap water	----	----	0.067±0.043	0.216±0.156	3.1	3.4	----	----
	0.1	0.1	0.164±0.090	0.312±0.183	3.3	2.6	97	96
Kan River	----	----	0.235±0.054	0.186±0.215	2.8	3.5	----	----
	0.1	0.1	0.333±0.059	0.281±0.147	2.5	3.6	98	95
Petrochemical factory waste water	----	----	0.345±0.112	0.052±0.035	2.5	2.7	----	----
	0.2	0.05	0.543±0.123	0.101±0.056	2.8	2.4	99	98
Well water	----	----	0.031±0.081	0.314±0.153	2.8	3.2	----	----
	0.05	0.25	0.080±0.053	0.567±0.175	2.5	3.4	98	101
Human serum 1	----	----	0.838±0.125	1.087±0.298	2.9	2.7	----	----
	1	1	1.822±0.091	2.101±0.248	2.8	3.2	98	101
Human serum 2	----	----	0.604±0.134	3.010±0.314	2.5	3.1	----	----
	0.55	2.5	1.139±0.166	5.48±0.395	2.8	3.5	97	99
Human urine 1	----	----	0.548±0.076	1.334±0.310	2.7	3.4	----	----
	1	1	1.532±0.113	2.288±0.270	2.5	2.9	98	95
Human urine 2	----	----	3.142±0.201	0.410±0.154	2.5	3.1	----	----
	2.5	0.35	5.575±0.342	0.753±0.171	2.9	3.5	97	98

[a] Mean of three determinations ± confidence interval (P = 0.95, n =5), [b] Relative standard deviation.

Table 5 Validation of developed L-US-D-μ-SPE method with Standard Reference Material (sample volume 5 mL; pH 3.5; sorbent 3 mg; extraction time 1 min, eluent 1000 μL of 0.3 mol L^{-1} NaOH)

sample	Certified ($\mu g\ L^{-1}$)		Added ($\mu g\ L^{-1}$)		Found [a] ($\mu g\ L^{-1}$)		Recovery (%)	
	As(V)	As(III)	As(V)	As(III)	As(V)	As(III)	As(V)	As(III)
NIST, SRM 2669[b]	2.41±0.30	1.47±0.10	----	----	2.37±0.13	1.48±0.11	98	101
			1.0	1.0	3.38±0.15	2.45±0.14	97	98

[a] Mean of three determinations ± confidence interval (P = 0.95, n =5),
[b] NIST, SRM 2669, level 1, arsenic species in frozen human urine, -20 ºC (p=0.95).

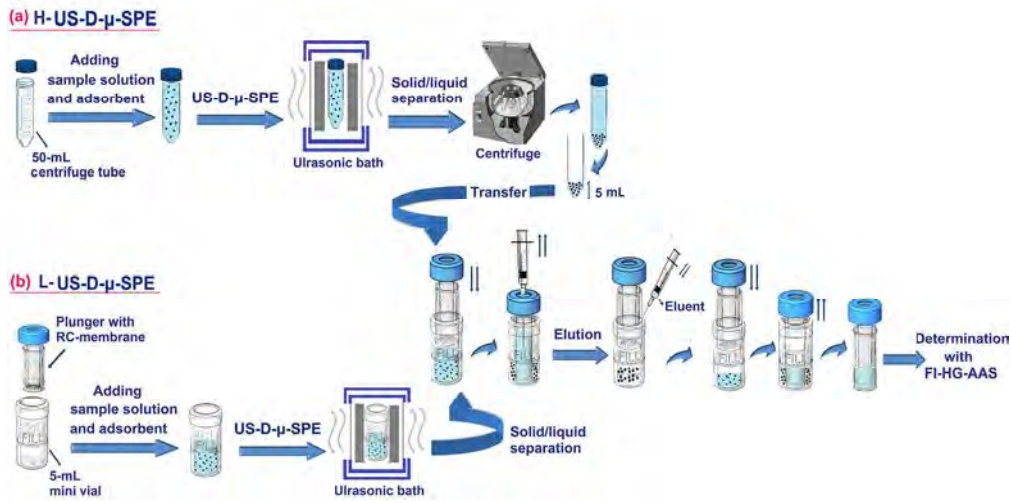

Fig. 1 Schematic setup for the carboxylated nanoporous graphene-based US-D-μ-SPE procedures. (a) H-US-D-μ-SPE and (b) L-US-D-μ-SPE.
170x85mm (300 x 300 DPI)

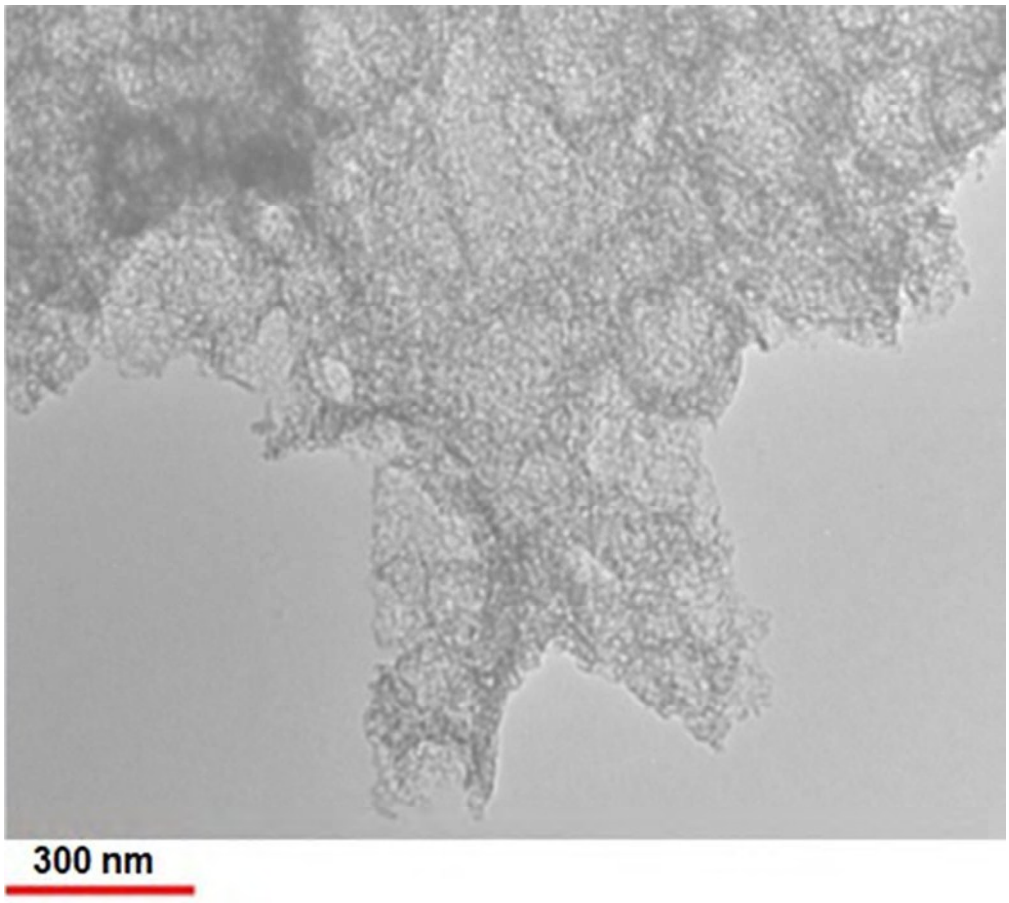

Fig. 2 (a) TEM image image of carboxylated nanoporous graphene.
82x74mm (300 x 300 DPI)

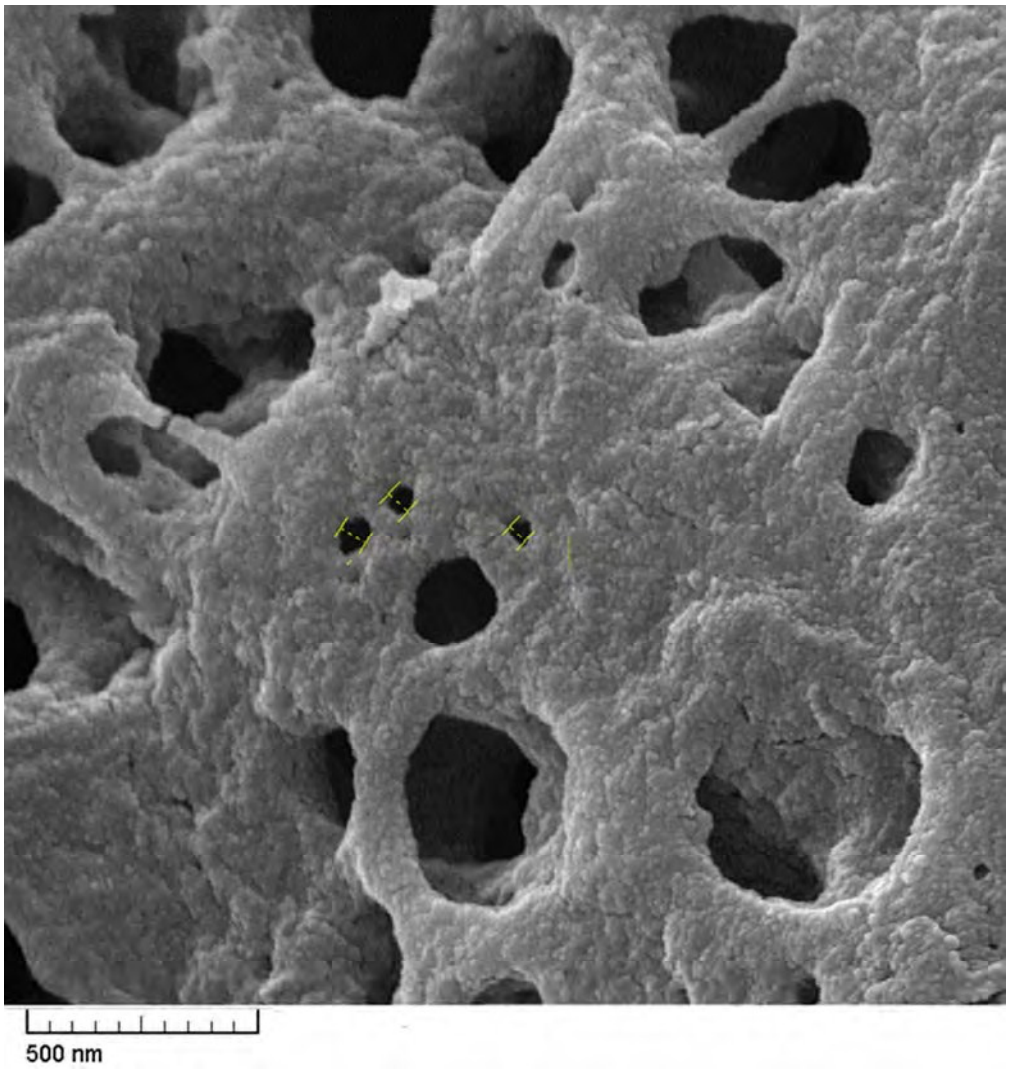

Fig. 2 (b) SEM image of carboxylated nanoporous graphene.
82x88mm (300 x 300 DPI)

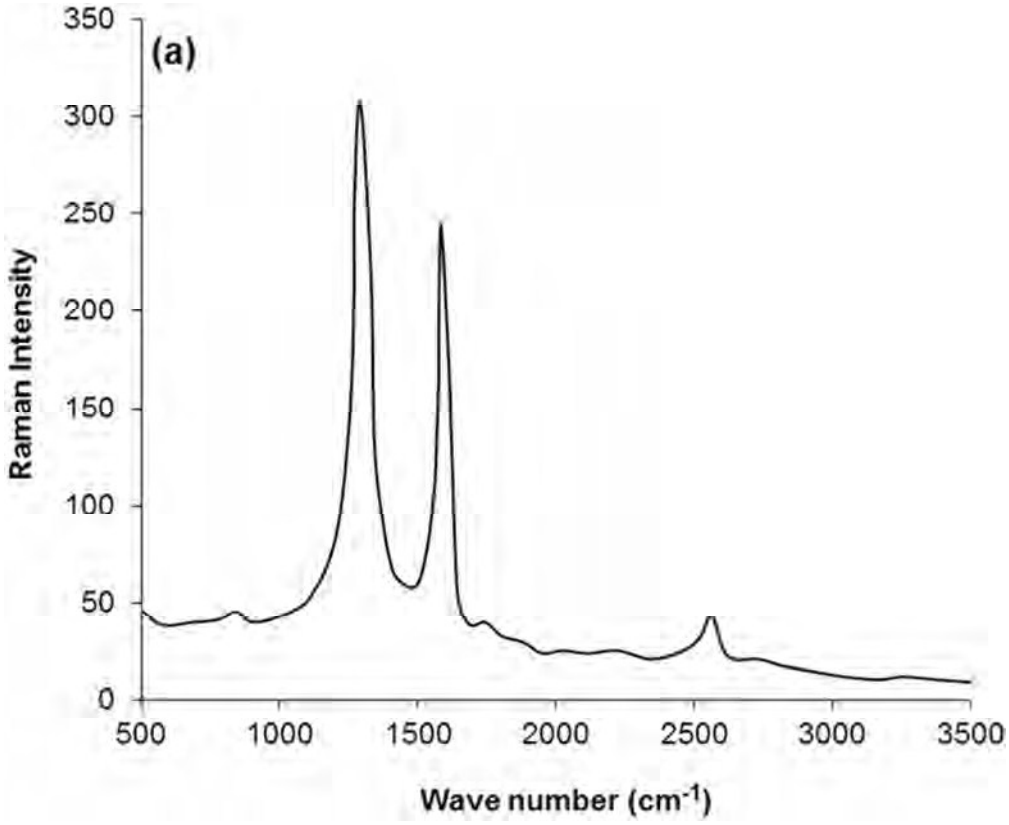

Fig. 3 (a) Raman spectra of pristine nanoporous graphene
82x67mm (300 x 300 DPI)

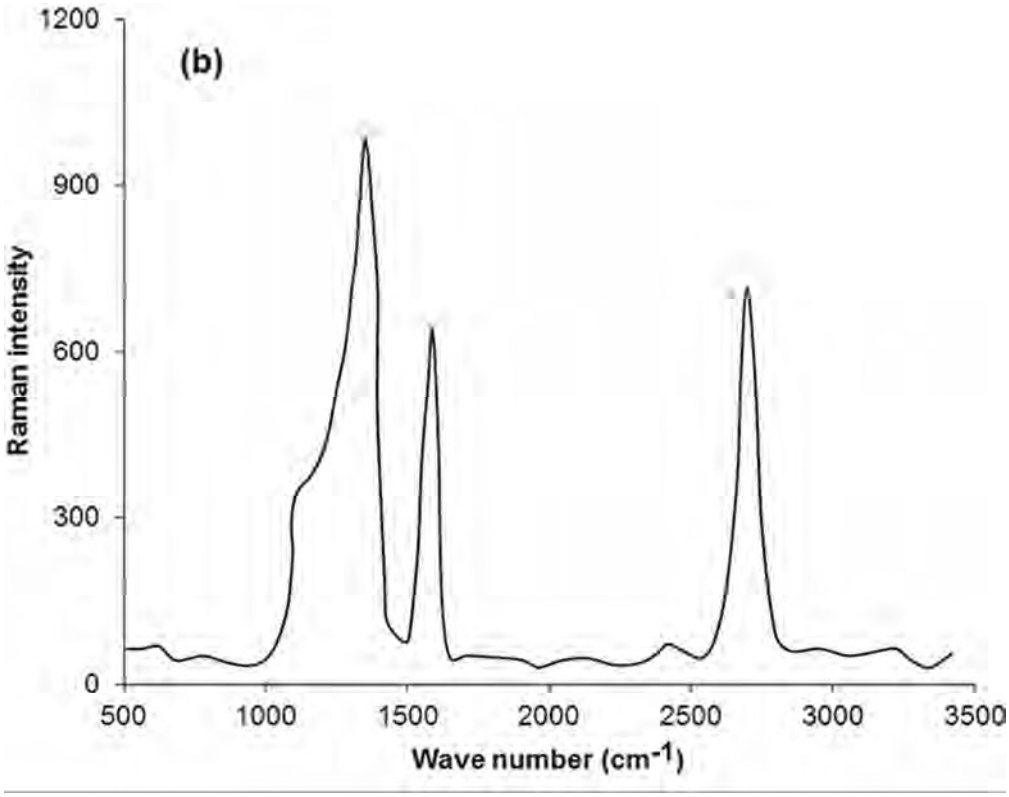

Fig. 3(b) Raman spectra of carboxylated nanoporous graphene.
82x65mm (300 x 300 DPI)

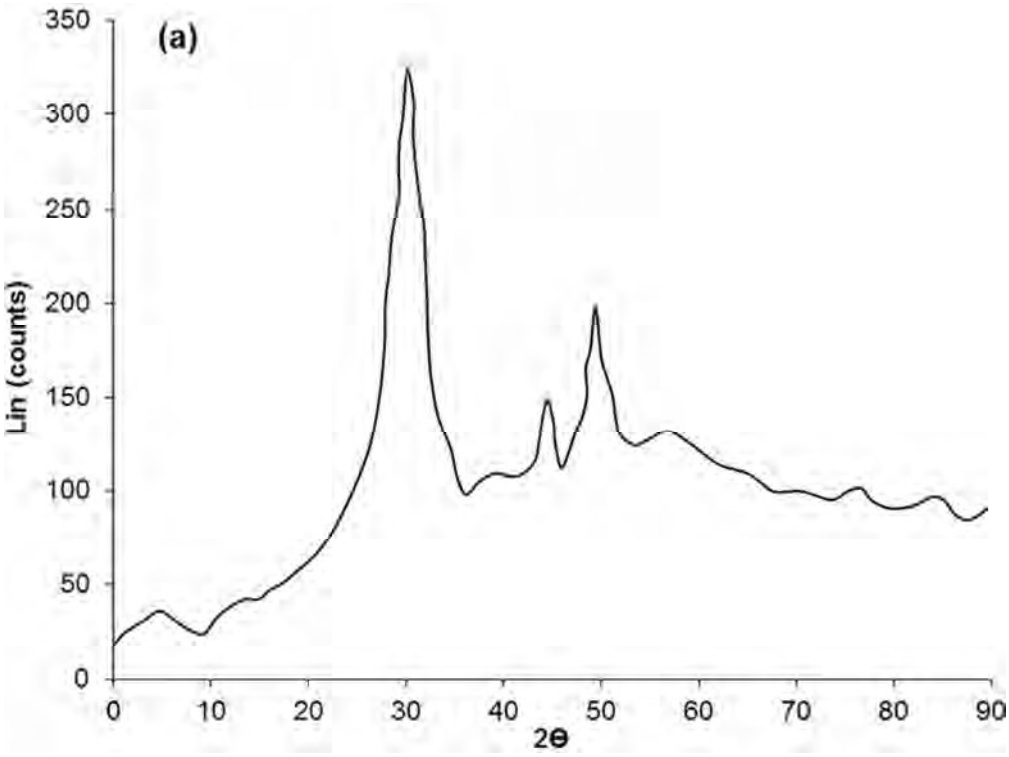

Fig. 4(a) XRD patterns of pristine nanoporous graphene
82x62mm (300 x 300 DPI)

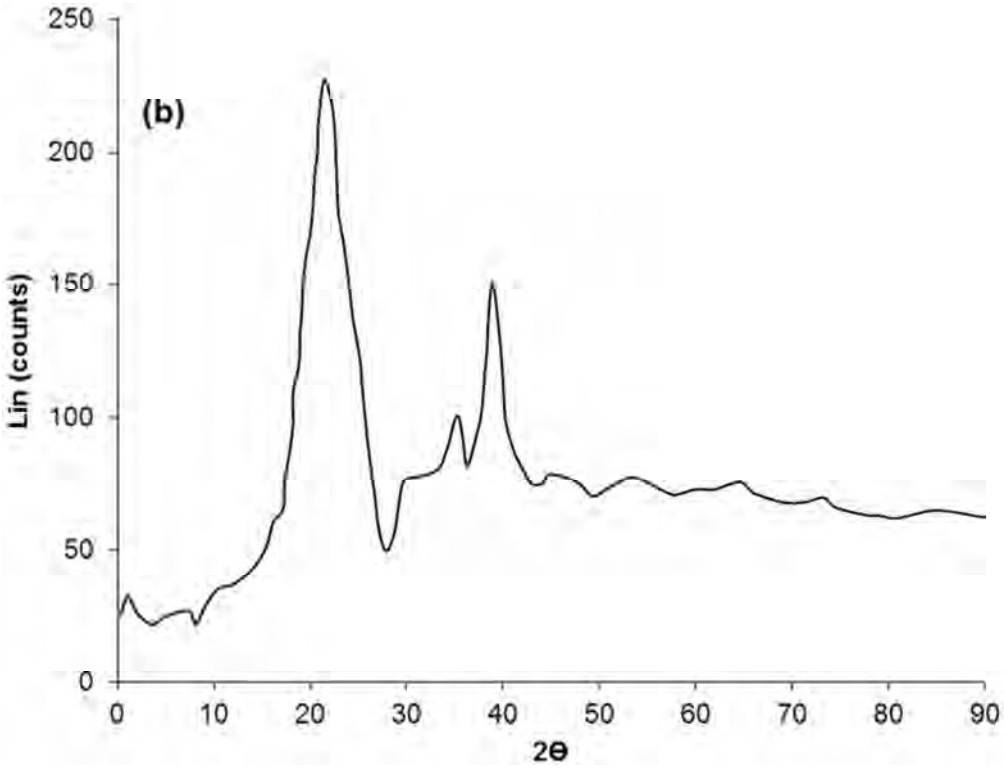

Fig. 4 (b) XRD patterns of carboxylated nanoporous graphene.
82x63mm (300 x 300 DPI)

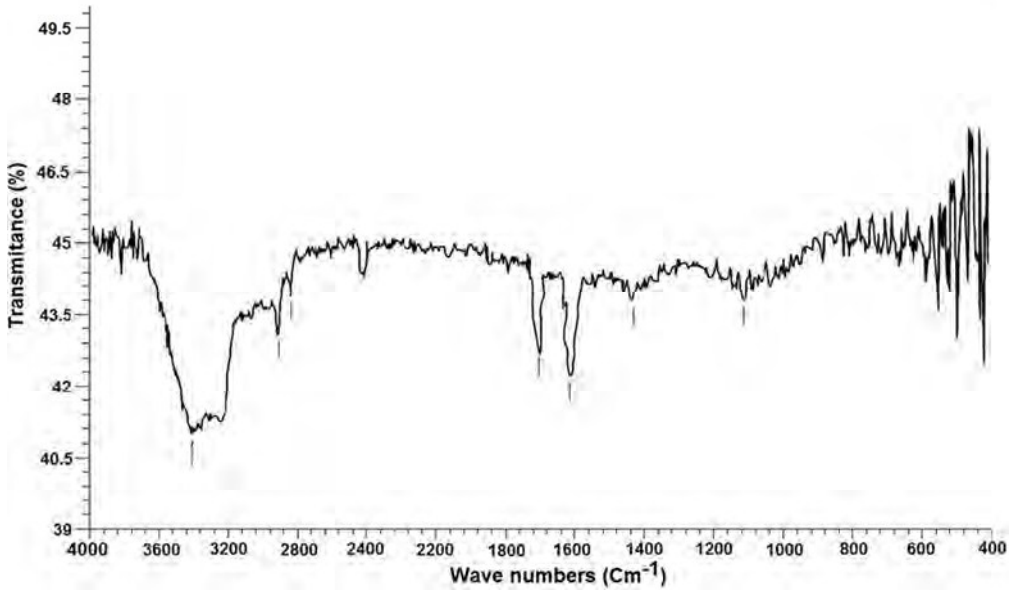

Fig. 5 FT-IR spectrum of carboxylated nanoporous graphene.
82x49mm (300 x 300 DPI)

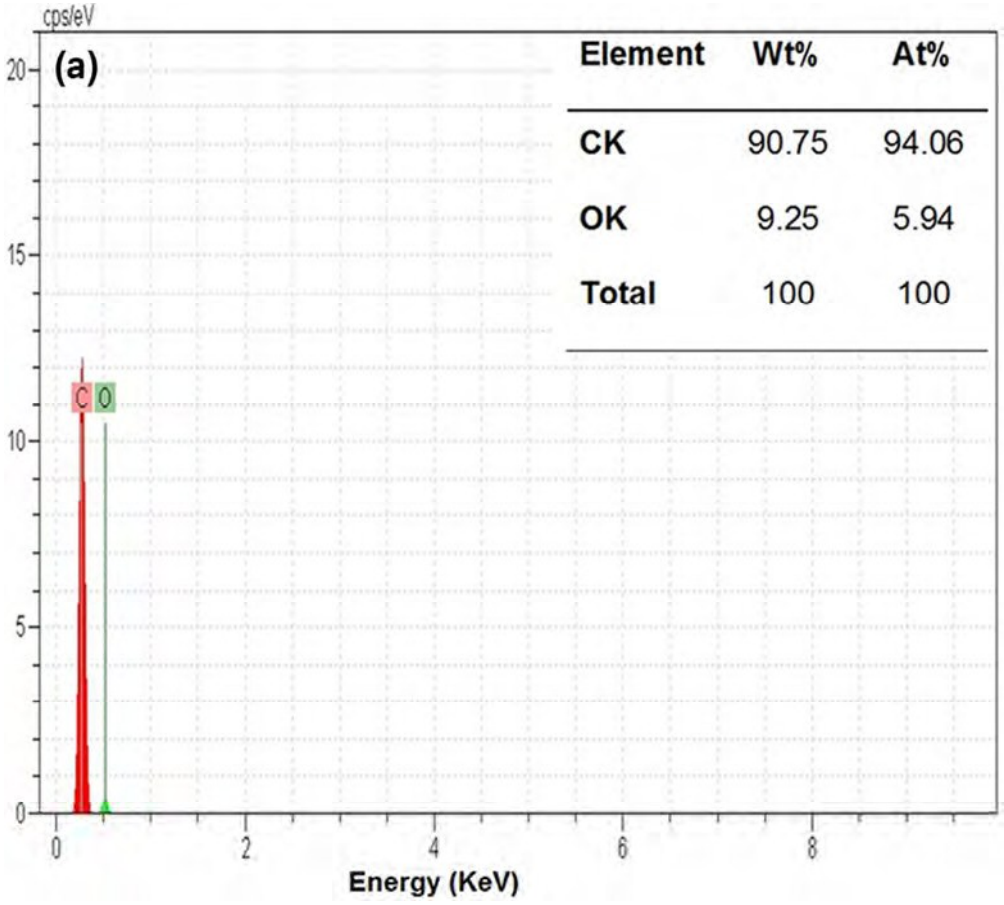

Fig. 6 (a) EDX spectra of pristine nanoporous graphene
82x74mm (300 x 300 DPI)

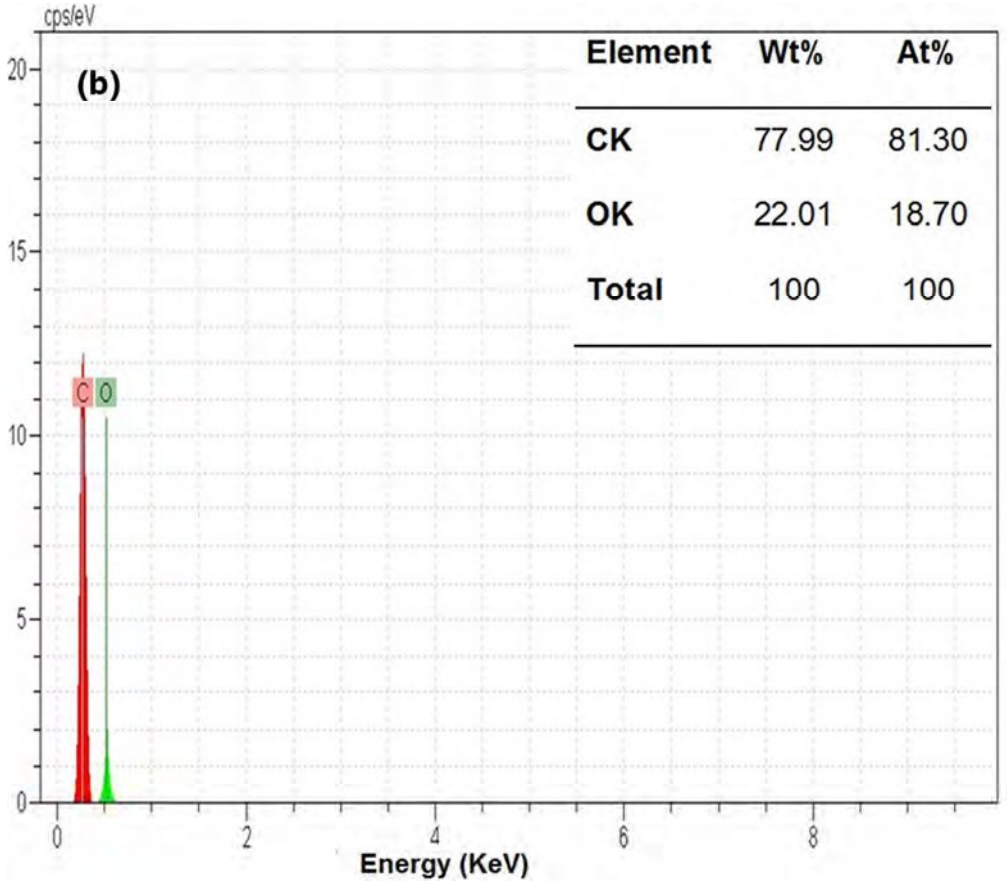

Fig. 6 (b) EDX spectra of carboxylated nanoporous graphene.
82x72mm (300 x 300 DPI)

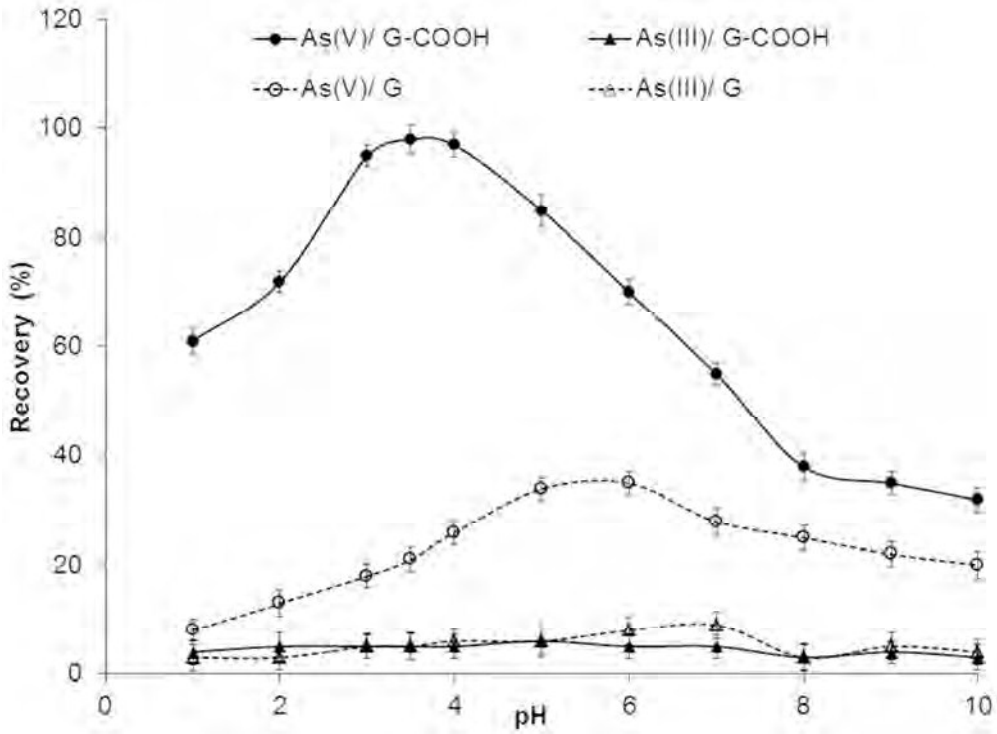

Fig. 7 Effect of solution pH on the recovery of 0.5 µg L-1 of As (III) and As (V) ions. Conditions. sample volume 50 mL; sorbent 10 mg; eluent 1000 µL of 0.5 mol L-1 NaOH; extraction time 3 min.
82x60mm (300 x 300 DPI)

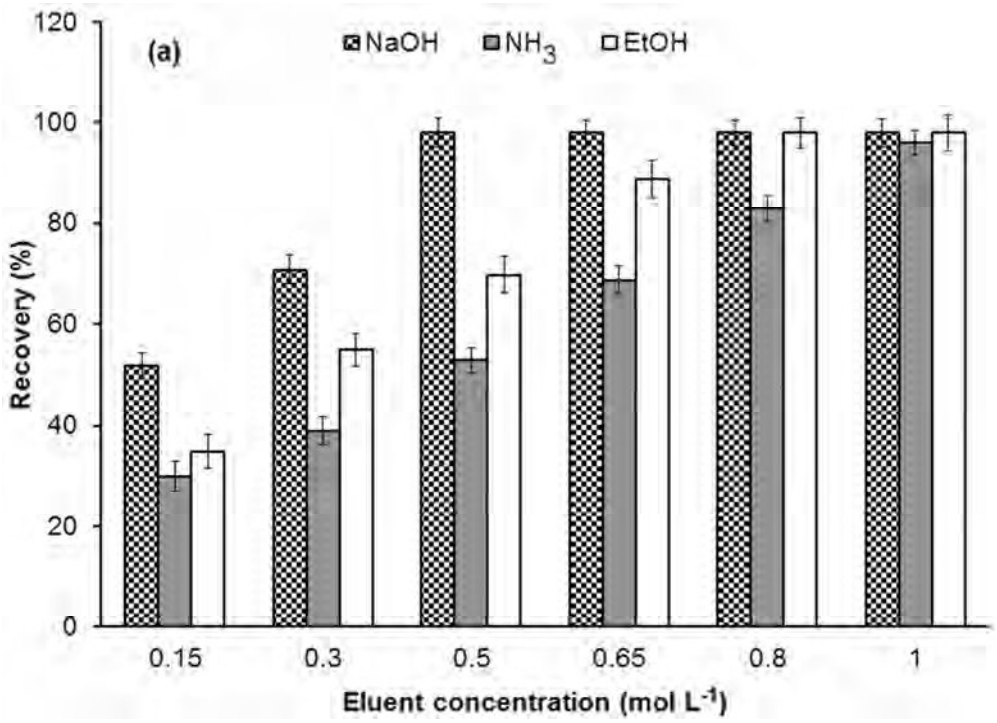

Fig. 8 Effect of eluent type and concentration on the recovery of 0.5 µg L-1 of As (V) ions. Conditions. solution pH 3.5; (a) H-US-D-µ-SPE: sample volume 50 mL; sorbent 10 mg; eluent volume 1000 µL; extraction time 3 min.
82x59mm (300 x 300 DPI)

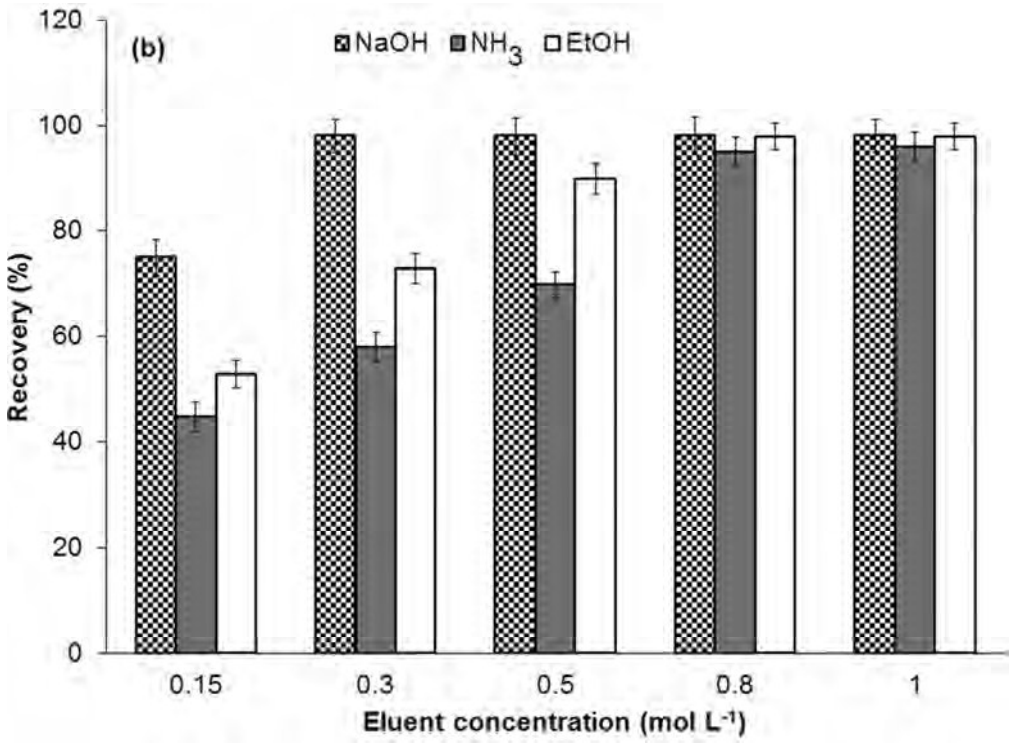

Fig. 8 Effect of eluent type and concentration on the recovery of 0.5 µg L-1 of As (V) ions. Conditions. solution pH 3.5;(b) L-US-D-µ-SPE: sample volume 5 mL; sorbent 3 mg; eluent volume 1000 µL; extraction time 1 min.
82x60mm (300 x 300 DPI)

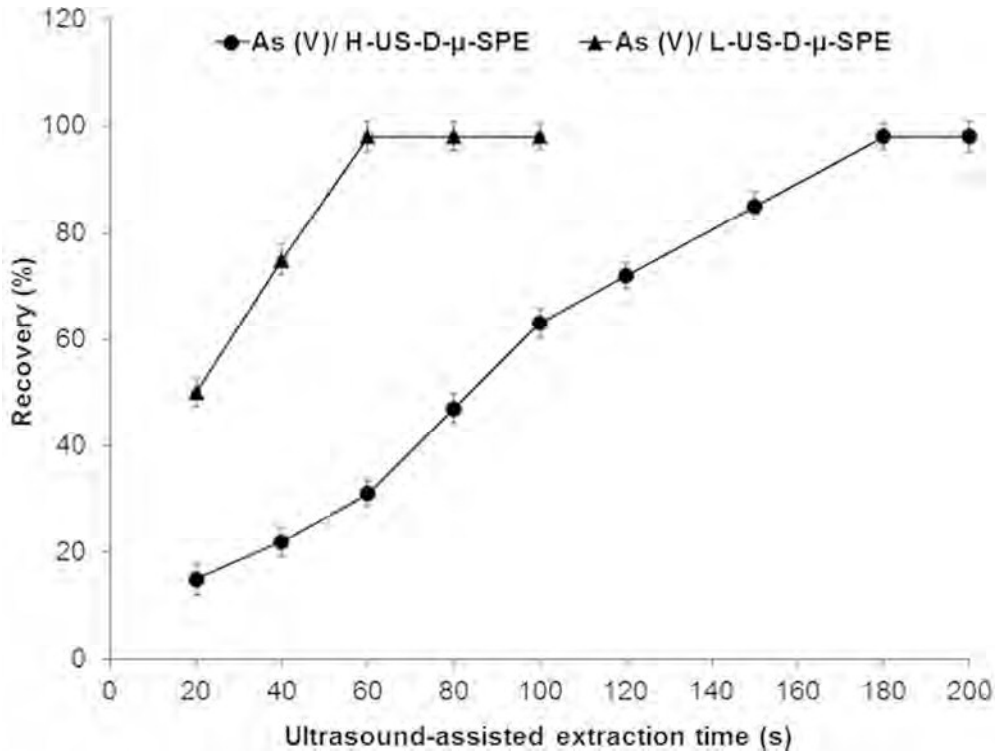

Fig. 9 Effect of ultrasonication time on the recovery of 0.5 μg L-1 of As (V) ions. Conditions. solution pH 3.5; (a) H-US-D-μ-SPE: sample volume 50 mL; sorbent 10 mg; eluent 1000 μL of 0.5 mol L-1 NaOH. (b) L-US-D-μ-SPE: sample volume 5 mL; sorbent 3 mg; eluent 1000 μL of 0.3 mol L-1 NaOH.
82x61mm (300 x 300 DPI)

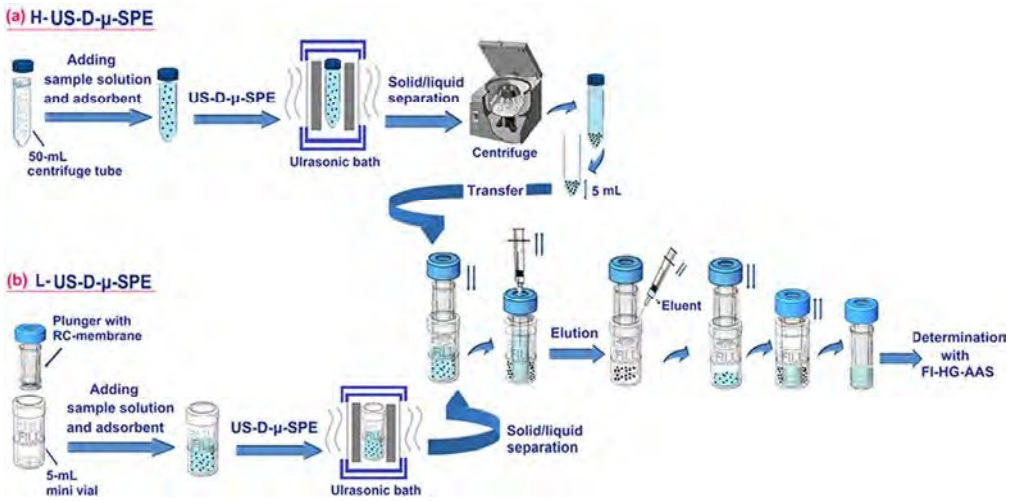

Graphical Abstract
80x39mm (300 x 300 DPI)